

## Enhancing approach of dispersion-compensation for dual-concentric-core photonic crystal fibers

Jui-Ming Hsu<sup>1,2\*</sup>, Che-Wei Yao<sup>1</sup> & Wei-Hsiang Chuang<sup>1</sup>

<sup>1</sup>Department of Electro-Optical Engineering, National United University, Miaoli, Taiwan 360, ROC

<sup>2</sup>Optoelectronics Research Center, National United University, Miaoli, Taiwan 360, ROC

E-mail: jmhsu@nuu.edu.tw

Received 6 February 2014; revised 20 May 2014; accepted 22 December 2014

An approach for enhancing the dispersion-compensation of dual-concentric-core photonic crystal fiber (DCC-PCF) is theoretically investigated. By enlarging the holes of inner cladding in order to increase the slope difference of index-curves between two supermodes, the negative chromatic dispersion coefficient is significantly enlarged. The reason of the approach is theoretically discussed in the present paper. The results indicate that the negative chromatic dispersion coefficient for the improved DCC-PCF using this approach is approximately 1.43 times greater than that of the previous work at around a wavelength of 1550 nm. Moreover, the confinement loss is estimated to verify that the loss of the improved DCC-PCF is extremely small.

**Keywords:** Photonic crystal, Chromatic dispersion, Optical communication

### 1 Introduction

Chromatic dispersion in single mode fibers (SMFs) induces temporal optical pulse broadening, resulting in serious restrictions in the data rates of high-speed optical communication links. The chromatic dispersion coefficient  $D$  is used to quantify the amount of chromatic dispersion.  $D$  is defined as<sup>1</sup>:

$$D = -\frac{\lambda}{c} \frac{d^2 n_{\text{eff}}}{d\lambda^2} \quad \dots(1)$$

where  $\lambda$  represents the operating wavelength,  $c$  the speed of light in a vacuum and  $n_{\text{eff}}$  is the effective indices of the fundamental guided modes on a fiber at various wavelengths. Currently, dispersion-compensating fibers (DCFs) are extensively used in optical fiber communication systems to minimize the negative effects of chromatic dispersion. The absolute dispersion value of conventional DCFs over the step index design<sup>2</sup> was probably hundreds of ps/nm-km. It is known that the larger the magnitude of the negative dispersion value of DCF at the transmission wavelength, the shorter will be the required DCF to compensate the dispersion resulted in a SMF and therefore, the lower will be the additional losses and non-linearity.

Auguste *et al.*<sup>3</sup> reported a conventional modified chemical vapour deposition (MCVD) DCF while

using a dual-concentric-core fiber (DCCF) structure with a high dispersion coefficient of  $-1800$  ps/(nm-km). Jerome *et al.*<sup>4</sup> decreased the air hole size of the fourth layer of index-guiding photonic crystal fiber (PCF) to achieve a dual-concentric core photonic crystal fiber (DCC-PCF), the dispersion coefficient of their DCC-PCF increased up to  $-2200$  ps/(nm-km) at a wavelength of 1550 nm. Additional research involved altering the air hole size of a specific layer<sup>5-9</sup> of PCFs to design DCC-PCFs. These research works are all based on a DCCF structure, which is given the large magnitude of the negative chromatic dispersion coefficient-effectively compensate for the considerable positive dispersion in long-distance fiber networks.

In the present paper, an approach for increasing the magnitude of the negative dispersion value of DCC-PCF is proposed. To increase the negative dispersion coefficient, the slope difference of index-curves between two supermodes at the transmission wavelength must be raised. The manner of raising the slope difference is quite easy; just simply enlarge the holes of inner cladding. The theories have been discussed and furthermore a numerical example of dispersion coefficient and confinement loss for some improved structure has been estimated and compared with a previous work<sup>4</sup>.

**2 Theoretical Model and Numeric Results**

The DCCF (Ref. 3) and DCC-PCFs in Refs 4-9 are composed of two concentric cores to propagate two supermodes. These supermodes, referred to as inner and outer mode, are characterized by a strong spatial redistribution of their modal fields as the wavelength varies. The cross-sectional view of the previous reported structure<sup>4</sup> (type I) and the improved structure using the approach proposed in the present (type II) are shown in Fig. 1(a and b), respectively. The cladding of these two types of DCC-PCF all consist of a triangular lattice of air holes with a pitch (center-to-center distance between the holes) of  $\Lambda$  in a background of undoped silica, whose refractive index can be estimated using the Sellmeier equation<sup>10</sup>:

$$n(\lambda) = \left[ 1 + \frac{0.6961663\lambda^2}{\lambda^2 - (0.0684043)^2} + \frac{0.4079426\lambda^2}{\lambda^2 - (0.1162414)^2} + \frac{0.8974794\lambda^2}{\lambda^2 - (9.896161)^2} \right]^{1/2} \dots(2)$$

The solid core is formed by removing a central air hole. The fourth layer of smaller-diameter air holes (diameter of  $\phi$ ), which define the outer ring core (ORC), separate the cladding region into inner cladding (consisting of air holes with a diameter of  $d_1$ ) and outer cladding (consisting of air holes with a diameter of  $d_2$ ). The theory of DCC-PCF structure has been described in detail in previous work<sup>4</sup>. The central guide comprising the solid core and inner cladding propagates the inner mode. Furthermore, the outer guide composed of the ORC and the inner and outer cladding propagates the outer mode. Figure 2

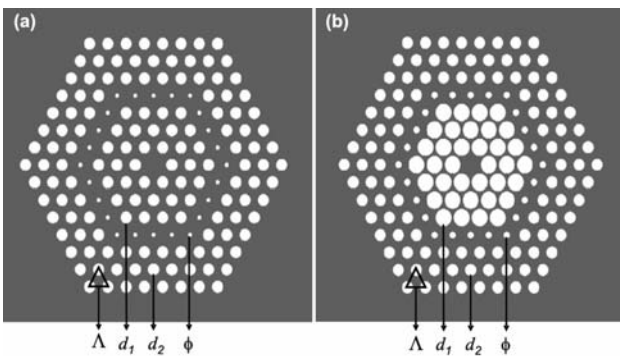


Fig. 1 — Cross-sectional view of the dual-concentric-core dispersion compensation photonic crystal fibers for (a) type I (previous structure) and (b) type II (improved structure)

shows that the effective indices of these two modes are equal at the phase-matching wavelength  $\lambda_o$ . The fundamental mode coincides with the inner mode at wavelengths shorter than  $\lambda_o$ ; thus, the propagation field is essentially confined within the central core at these wavelengths. At wavelengths longer than  $\lambda_o$ , the fundamental mode switches to the outer mode, meaning that most of the power is effectively guided to the ORC. At the wavelength of  $\lambda_o$ , an abrupt break is occurred for the effective-index curve of the fundamental mode.

According to Eq. (1),  $d^2n_{eff}/d\lambda^2$  signifies the curvature of the index curve of the fundamental mode in Fig. 2. In other words, the chromatic dispersion coefficient  $D$  at  $\lambda_o$  signifies the transient rate of break (i.e., the slope difference between curves of effective indices of the inner and outer modes). Therefore, the slope difference at  $\lambda_o$  directly determines the magnitude of  $D$ .

Figure 3 shows the dependence of the effective indices on wavelength for the two kinds of PCF with different size of cladding holes. The index curve of fiber B (with larger cladding holes) should be steeper than that of fiber A (Fig. 3). This can be explained as follows. For the modes of wavelength  $\lambda \ll \Lambda$ , the effective indices approximate to the index of silica, regardless of whether fiber A or B is used. Therefore, two index curves are close to each other in a short wavelength region. For the modes of longer wavelength  $\lambda \gg \Lambda$ , the effective indices can be regarded as the average of index of material filled in holes (air in this case) and the background (silica); the  $n_{eff}$  must be lower for the case of larger cladding holes (fiber B). The central guides of the DCC-PCFs shown

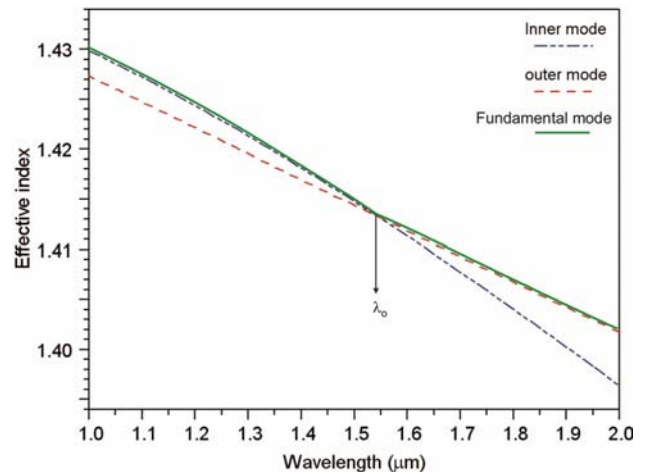


Fig. 2 — Effective indices versus wavelengths

in Fig. 1(a and b), are equivalent to the PCFs as shown in Fig. 3. Therefore, to enlarge the slope difference, the diameter of inner cladding holes can be increased as indicated in Fig. 1(b). In the present, DCC-PCF type I [Fig. 1(a)] with a diameter of fourth-layer air holes of  $\phi=0.51 \mu\text{m}$ , a diameter of cladding holes  $d_1=d_2=1.4 \mu\text{m}$ , and a pitch of  $\Lambda=2.3 \mu\text{m}$  (Ref. 4) as well as DCC-PCF type II [Fig. 1(b)] with a diameter of fourth-layer air holes of  $\phi=0.80 \mu\text{m}$ , the diameters of cladding holes  $d_1=2.0 \mu\text{m}$  and  $d_2=1.4 \mu\text{m}$ , and a pitch of  $\Lambda=2.3 \mu\text{m}$  (proposed structure) are simulated using the plane-wave expansion (PWE) method to estimate the effective refractive index ( $n_{\text{eff}}$ ) of fundamental mode, the dispersion coefficient  $D$  is then evaluated by substituting  $n_{\text{eff}}$  into Eq. (1). Figure 4 shows the relation of the effective indices versus wavelength for DCC-PCF of both types I and II. In substance, the index curve of the inner mode of type II is considerably steeper than that of type I. However, the outer mode curve of type II is slightly steeper than that of type I. Thus, the slope difference and the chromatic dispersion coefficient  $D$  of DCC-PCF type II are expectantly larger than that of DCC-PCF type I.

Moreover, a typical refractive index profile<sup>11</sup> of traditional DCFs is shown in Fig. 5. This index profile happens to agree with the effective index distribution of the proposed structure. In the proposed DCC-PCF (type II), as shown in Fig. 1(b), the pure-silica inner

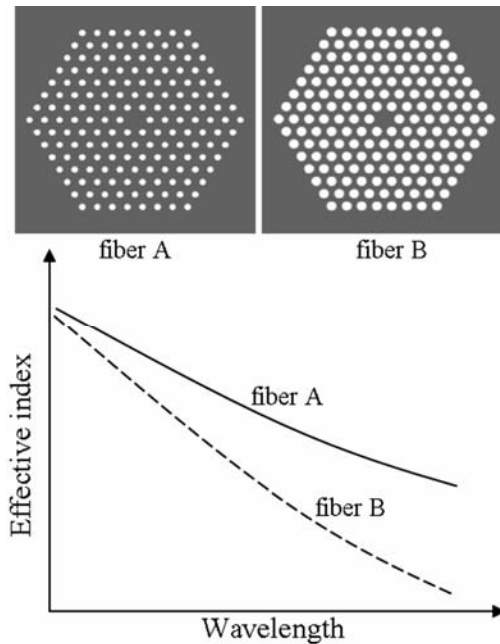


Fig. 3 — Dependence of the effective indices on wavelengths for photonic crystal fibers with different size of cladding holes

core with highest index corresponds to the inner core of DCF with an index of  $n_{\text{corin}}$ . The inner cladding region with a larger air hole (lowest effective index) corresponds to the inner cladding of DCF with an index of  $n_{\text{cldin}}$ . The ORC with the smallest air hole (higher effective index) corresponds to the outer core of DCF with the index of  $n_{\text{corout}}$ . Finally, the outer cladding region is the corresponding area of the outer cladding of DCF with the index of  $n_{\text{clout}}$ .

The diameter of fourth-layer air holes  $\phi$  can be used to fine-tune the phase-matching wavelength  $\lambda_o$ .

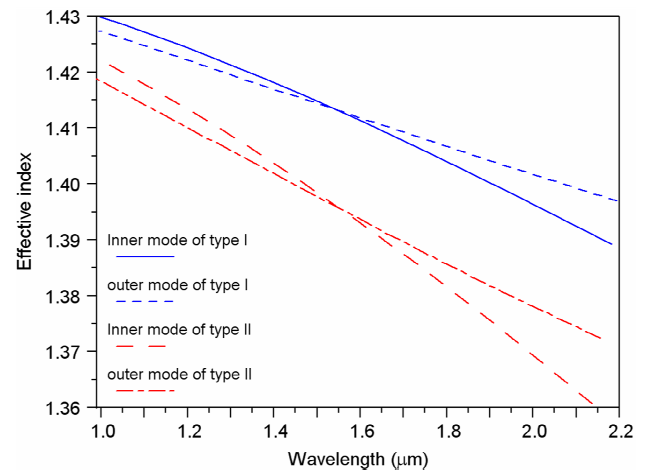


Fig. 4 — Relation of the effective indices versus wavelengths for DCC-PCF of type I ( $d_1=d_2=1.4 \mu\text{m}$ ,  $\phi=0.51 \mu\text{m}$ ) and type II ( $d_1=2.0 \mu\text{m}$ ,  $d_2=1.4 \mu\text{m}$ ,  $\phi=0.80 \mu\text{m}$ ).  $\Lambda=2.3 \mu\text{m}$  for both types

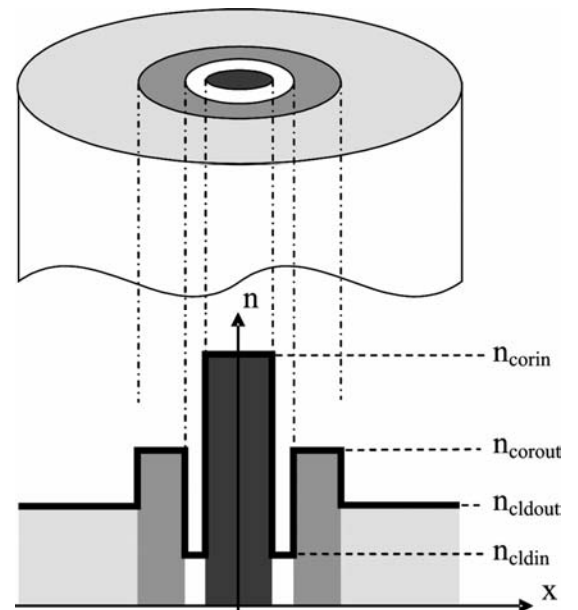


Fig. 5 — Typical refractive index profile of traditional dispersion-compensating fibers

Figure 6 shows the dependence of the effective indices on wavelength for the inner mode and outer modes of DCC-PCF type II with various diameters  $\phi$  of the fourth-layer air holes. The simulations as shown in Fig. 6 use the same geometric parameters of DCC-PCF type II ( $\Lambda=2.3 \mu\text{m}$ ,  $d_1=2.0 \mu\text{m}$ ,  $d_2=1.4 \mu\text{m}$ ). In the case of  $\phi=0.51 \mu\text{m}$  (the same fourth-layer air holes diameter as type I), the phase-matching wavelength  $\lambda_o$  which is the intersection of the index-curves of inner and outer modes, is shorter than 1000 nm. This phenomenon is due to a fact that the effective indices of inner mode are significantly decreased while those of outer mode are changeless for increasing inner cladding holes. To shift the  $\lambda_o$  to a wavelength closer to the habitual wavelength of optical-fiber communications (1550 nm),  $\phi$  must be increased as a larger  $\phi$  increases the space-filling fraction and subsequently reduced the effective index of the outer mode. As shown in Fig. 6, the phase-matching wavelength shifts to a longer wavelength when the effective index of the outer mode is reduced. In the case of  $\phi=0.80 \mu\text{m}$ , the phase-matching wavelength  $\lambda_o$  is approximately 1561 nm, which is used in the improved structure in Fig. 1(b).

Figure 7 shows the dependence of the estimated chromatic dispersion coefficient  $D$  on the wavelength for the DCC-PCFs with  $d_1=2.0 \mu\text{m}$  (type II),  $1.9 \mu\text{m}$ ,  $1.8 \mu\text{m}$  and  $1.4 \mu\text{m}$  (type I). To shift the compensation wavelength to a wavelength closer to 1550 nm, the hole-diameter of ORC in each DCC-PCF structures are designed as  $\phi=0.800, 0.738, 0.681$  and  $0.510 \mu\text{m}$ ,

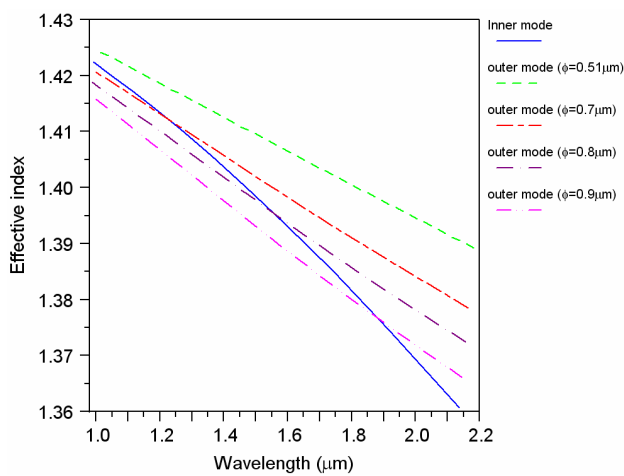


Fig. 6 — Dependence of the effective indices on wavelengths for inner and outer modes using various diameters  $\phi$  of the fourth-layer air holes.  $\Lambda=2.3 \mu\text{m}$ ,  $d_1=2.0 \mu\text{m}$ ,  $d_2=1.4 \mu\text{m}$  (DCC-PCF type II)

respectively. The corresponding parameters of these structures are summarized in Table 1. Comparing two types of DCC-PCF as shown in Fig. 1, DCC-PCF type I has a minimum chromatic dispersion of  $D \approx -2541 \text{ ps}/(\text{km}\cdot\text{nm})$  at a wavelength of 1544 nm whereas DCC-PCF type II has a minimum chromatic dispersion of  $D \approx -3633 \text{ ps}/(\text{km}\cdot\text{nm})$  at a wavelength of 1561 nm. Thus, the negative chromatic dispersion of the improved structure is approximately 1.43 times larger than the former.

The avoid crossing phenomenon of the fundamental mode in Fig. 2 results in a large negative dispersion. However, one may concern that it probably brings about a comparably large loss simultaneously. Therefore, the confinement losses of some DCC-PCF structure are studied in this work. The confinement loss ( $L_c$ ) for each structure is deduced by the value of the imaginary part of effective indices ( $n_{\text{eff}}$ ) as:

$$L_c = 8.686 \times k_o \times \text{Im}[n_{\text{eff}}] \quad \dots(3)$$

where  $k_o$  is the free-space wave number and  $\text{Im}[n_{\text{eff}}]$  represents the imaginary part of  $n_{\text{eff}}$ . The numeric results of the confinement loss at around a wavelength of 1550 nm for each structure are generalized in Table 1. It is obvious in Table 1, the confinement loss of the DCC-PCFs with larger inner cladding holes ( $d_1 = 1.8, 1.9$  and  $2.0 \mu\text{m}$ , respectively) are all too small to consider. In conclusion, by appropriately enlarging

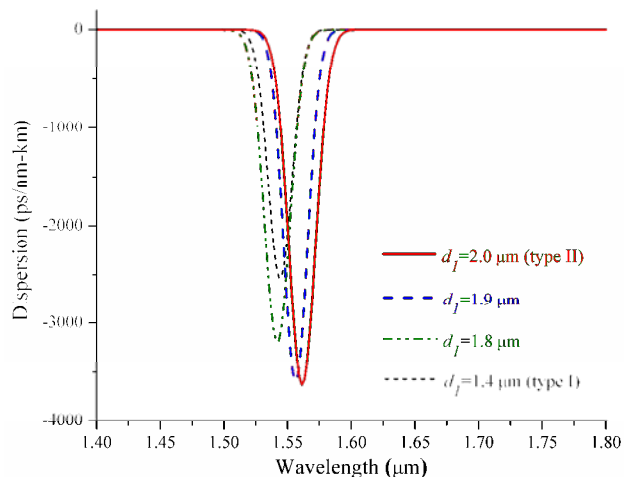


Fig. 7 — Dependence of the estimated chromatic dispersion coefficient  $D$  on wavelengths for DCC-PCFs with  $d_1=2.0 \mu\text{m}$  ( $\phi=0.800 \mu\text{m}$ , type II),  $d_1=1.9 \mu\text{m}$  ( $\phi=0.738 \mu\text{m}$ ),  $d_1=1.8 \mu\text{m}$  ( $\phi=0.681 \mu\text{m}$ ) and  $d_1=1.4 \mu\text{m}$  ( $\phi=0.510 \mu\text{m}$ , type I).  $\Lambda=2.3 \mu\text{m}$ ,  $d_2=1.4 \mu\text{m}$  in each type of DCC-PCF

Table 1 — Dispersion and confinement loss for the DCC-PCFs with a different diameter of inner cladding ( $d_1$ ) at around a wavelength of 1550 nm

$A$ ( $\mu\text{m}$ )					2.3
$d_2$ ( $\mu\text{m}$ )					1.4
$d_1$ ( $\mu\text{m}$ )	1.4 (type I)	1.8	1.9	2.0 (type II)	
$\phi$ ( $\mu\text{m}$ )	0.510	0.681	0.738	0.800	
Compensation wavelength (nm)	1544	1542	1556	1561	
Dispersion (ps/nm-km)	-2541	-3201	-3607	-3633	
Confinement loss (dB/km)	$3.93 \times 10^{-4}$	$9.39 \times 10^{-8}$	$3.13 \times 10^{-9}$	$5.40 \times 10^{-7}$	

the holes of inner cladding, we can achieve a DCC-PCF with a larger negative dispersion and a negligible confinement loss.

### 3 Conclusions

This work has theoretically derived that the holes of inner cladding in a DCC-PCF structure can be enlarged to increase the negative chromatic dispersion coefficient and keep the propagation mode in low attenuation. The effective index distribution of the proposed structure happens to agree with a typical refractive index profile of traditional dispersion-compensating fibers completely. The numeric results indicate that the negative chromatic dispersion coefficient for the improved DCC-PCF with  $d_1 = 2.0 \mu\text{m}$  is approximately 1.43 times greater than that of the previous work at around a wavelength of 1550 nm.

### References

- 1 Govind P Agrawal, *Nonlinear Fiber Optics* (Academic, New York), 2001.
- 2 Vengsarkar A M & Reed W A, *Opt Lett*, 18 (1993) 924.
- 3 Auguste J L, Blondy J M & Maury J *et al.*, *Opt Fiber Technol*, 8 (2002) 89.
- 4 Gerome F, Auguste J L & Blondy J M, *Opt Lett*, 29 (2004) 2725.
- 5 Ni Y, Zhang L & An L *et al.*, *IEEE Photon Technol Lett*, 16 (2004) 1516.
- 6 Varshney S K, Saitoh K & Koshiba M, *IEEE Photon Technol Lett*, 17 (2005) 2062.
- 7 Fujisawa T, Saitoh K, Wada K & Koshiba M, *Opt. Express*, 14 (2006) 893.
- 8 Subbaraman H, Ling T & Jiang Y *et al.*, *Appl Opt*, 46 (2007) 3263.
- 9 Zhao X, Zhou G & Li S *et al.*, *Appl Opt*, 47 (2008) 5190.
- 10 Malitson I H, *J Opt Soc Am*, 55 (1965) 1205.
- 11 Thyagarajan K & Ghatak A, *Fiber Optic Essentials* (John Wiley, New Jersey) 2007, p. 94.